Fusion Engineering and Design 193 (2023) 113688

Contents lists available at ScienceDirect

Fusion Engineering and Design

journal homepage: www.elsevier.com/locate/fusengdes

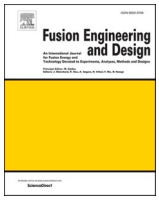

Thermal-hydraulic assessment of Once-Through Steam Generators for EU-DEMO WCLL Breeding Blanket primary cooling system application

C. Ciurluini [a,*], Alessandra Vannoni [a], Tommaso Del Moro [a], Pierdomenico Lorusso [b], Amelia Tincani [c], Alessandro Del Nevo [c], Luciana Barucca [d], Fabio Giannetti [a]

[a] DIAEE, Sapienza University of Rome, Corso Vittorio Emanuele II, 244, Roma 00186, Italy
[b] ENEA, Department of Fusion and Nuclear Safety Technology, Frascati, Rome I-00044, Italy
[c] ENEA Department of Fusion and Nuclear Safety Technology, Camugnano (BO) 40032, Italy
[d] Ansaldo Nucleare, Via N. Lorenzi 8, Genova 16152, Italy

ARTICLE INFO

Keywords:
OTSG
PHTS
RELAP5
Transient analysis
Balance of Plant
STEAM

ABSTRACT

Once-Through Steam Generators (OTSGs) were recently selected to be installed in the Primary Heat Transfer Systems (PHTS) related to EU-DEMO WCLL Breeding Blanket (BB). Referring to the Balance of Plant Direct Coupling Design (BoP-DCD) option, these components are used to deliver the thermal power removed from the two principal blanket subsystems, i.e. First Wall (FW) and Breeder Zone (BZ), to the Power Conversion System (PCS).

OTSG design foresees a vertical component with primary water moving downward inside tube bundle and secondary fluid flowing throughout shell in counter current. The latter moves firstly downwards through the annular downcomer and then goes up in the central riser, where it boils up to super-heated steam conditions. Then, it is deflected by the upper tubesheet, flows again downwards along the steam downcomer and exits through the laterally connected steam nozzles.

In the last years, as part of the research activities associated to the Work Package Balance of Plant (WPBoP), a detailed analysis of the steam generator, aimed at deeply understanding the main thermal-hydraulic aspects characterizing its performances during the pulsed regime of DEMO normal operations, was performed. To fulfil this scope, a complete model of the component was prepared by using the best-estimate system code RELAP5/MOD3.3, selected to be also the reference design verification tool.

During operations, OTSG experiences full-load and low-load alternative phases with rapid transitions from one another. The steam generator capability to follow such load variations avoiding the occurrence of instabilities in the component was studied. The computational activity carried out was a preliminary thermal-hydraulic characterization of the component conceptual design during both pulse and dwell phases. The feedbacks of this analysis were also fundamental for the conceptualization of the steam generator mock-up to be installed in the planned STEAM facility that will be built at the ENEA Research center of Brasimone.

1. Introduction

The European Demonstration Fusion Power Plant (EU-DEMO) is a very complex machine designed to fulfill different purposes. Among them, one of the most important is demonstrating the economic competitiveness of such kind of energy source with respect to the ones already present in the market. To reach this goal, the reactor must be provided with a Balance of Plant (BoP) to ensure that the thermal power removed from plasma is converted into electricity.

Within the framework of the EUROfusion Consortium research activities, different BoP design options are currently investigated, as widely discussed in Refs. [1,2]. System configuration strongly depends on the concept adopted for another reactor key component: the Breeding Blanket (BB). The latter acts as cooling device, tritium breeder and neutron shield. During past years, ENEA and its related partners, among which there is also the Department of Astronautical, Electrical and Energy Engineering (DIAEE) of Sapienza University of Rome, focused their research efforts on the Water-Cooled Lithium Lead (WCLL) BB solution,

* Corresponding author.
E-mail address: cristiano.ciurluini@uniroma1.it (C. Ciurluini).

https://doi.org/10.1016/j.fusengdes.2023.113688
Received 11 October 2022; Received in revised form 27 February 2023; Accepted 22 March 2023
Available online 27 March 2023

considered also in this paper. A detailed description of the WCLL blanket layout is available in Ref. [3]. For the purpose of the current discussion, what is worth to be noted is that it relies on water as coolant, liquid lead-lithium (PbLi) as breeder, neutron multiplier and tritium carrier and on EUROFER (EU) as structural material. Furthermore, the overall BB can be divided in two main subsystems: the breeder zone (BZ) and the first wall (FW). They are cooled by independent cooling systems, named Primary Heat Transfer Systems (PHTS), [1,2]. The first removes the thermal power generated in the breeder zone by the interactions between the lead-lithium and the neutrons emitted by the plasma or due to the interaction with the surrounding materials. The second cools the FW, subjected to the incident heat flux and the neutron wall load. PHTS circuits are part of the BOP architecture.

According to Refs. [1,2], the reference solution for the WCLL BoP is the Direct Coupling Design (DCD) with small Energy Storage System (ESS). In this design option, both BZ and FW PHTSs are directly connected to the Power Conversion System (PCS), delivering the removed thermal power for its conversion into electricity. The coupling between primary and secondary circuits is provided by four Once Through Steam Generators (OTSG), a pair of identical components for each PHTS.

In nuclear fission industry, OTSGs were developed by Babcock & Wilcox (B&W) Company for Pressurized Water Reactor (PWR) applications and operated for decades, [4–7]. During last years, this technology was selected to be installed in DEMO WCLL BB PHTS, [1,2]. The main reasons are: primary (PHTS) and secondary (PCS) water thermodynamic conditions are comparable with respect to the ones of a PWR; the low water inventory present in the steam generator enhances its responsivity, making the component more suitable with respect to the pulsed regime foreseen for DEMO normal operations (see Refs. [1,2]). From 2021, one of the principal research activities belonging to the Work Package Balance of Plant (WPBoP) consisted in the development of a conceptual design for BZ and FW OTSGs, [8]. Within this framework, DIAEE performed the Thermal-Hydraulic (TH) design of the components and carried out the analyses needed to fully characterize their TH behavior.

The first activity is widely described in Ref. [8] and only briefly recalled in § 2. Instead, the present paper focuses on the TH analyses performed on the BZ and FW OTSGs, gathered in § 3. Calculations were carried out by using the best-estimate system code RELAP5/MOD3.3, [9], selected to be also the reference design verification tool. A complete model of the steam generator was prepared, see § 3.1. Firstly, the component performances were simulated at full plasma power state, considering both Beginning of Life (BoL) and End of Life (EoL) conditions (§ 3.2). These results needed also to verify the OTSG TH design, [8]. To better characterize the steam generator behavior, sensitivity studies were performed on some selected design parameters, as discussed in § 3.3. Finally, a transient analysis was carried out investigating the OTSG performances at reduced power levels, § 3.4. The chosen power steps swing from 100% to 1% of rated value, covering all the component operative scenarios during DEMO normal operations. The steam generator capability to operate in a stable way at both full-load and low-load conditions is preliminarily evaluated, since this is a crucial aspect in the component design.

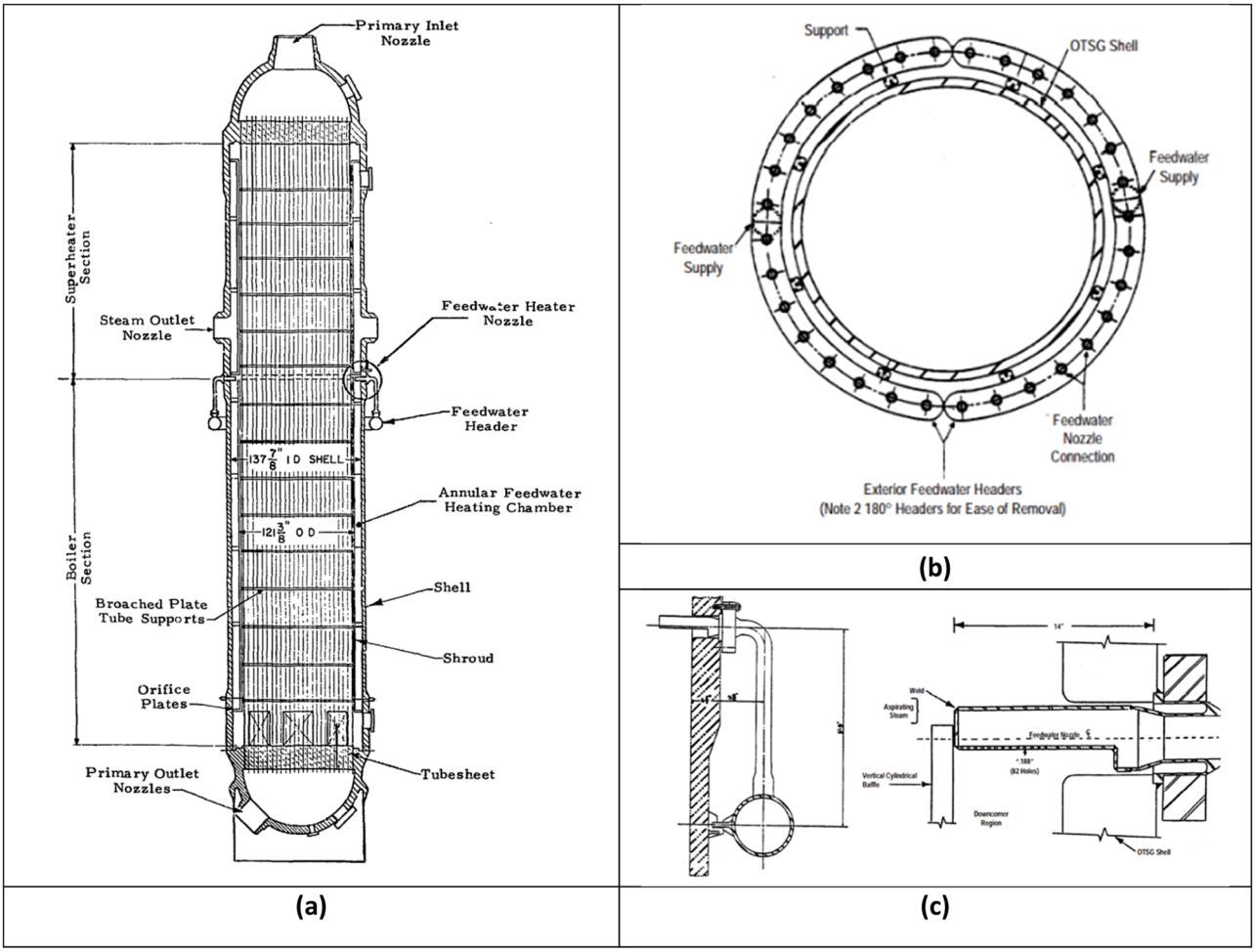

Fig. 1. OTSG technology, [5]: cross sectional view (a), feedwater inlet (b)–(c).

2. OTSG technology overview and BB PHTS steam generator conceptual design

The steam generator cross sectional view is shown in Fig. 1a, [5]. Primary system is bounded by the hemispherical heads, the tubesheets and the tube bundle. Primary coolant enters from the top and flows downwards, exiting from the component bottom. Instead, feedwater enters the OTSG through inlet nozzles connected to semi-circular headers located about midway along the shell (see Fig. 1b). Each inlet nozzle is equipped with holes, see Fig. 1c, through which feedwater is sprayed down into the annular heating chamber (also called lower downcomer) between the shell and the shroud (also named riser). Steam is aspirated from the high-quality region of the shroud, just above the feedwater nozzles. Steam flow preheats the feedwater, and the mixture arrives at the riser bottom nearly in saturated conditions. Steam flow is driven by the differential pressure between the shroud and the feedwater heating chamber. Such difference is due to the steam condensation occurring when the latter is mixed with the inlet feedwater. Saturated mixture enters the central riser thanks to water ports located just above the lower tubesheet. Then, it flows upwards along the central riser while heated up by the primary coolant. Secondary water boils up to dry steam and then is superheated. Once reached the top, steam is turned by the upper tubesheet and directed to the annulus between riser and vessel in the OTSG upper section (also named steam downcomer). Here, it flows downwards to the two outlet nozzles, connected laterally just above the inlet ones. In this way, the upper portion of the OTSG is bathed in superheated steam while the lower in saturated water.

As stated above, one of the DIAEE main activities within the framework of FP9 WPBoP was the development of a thermal-hydraulic conceptual design for the BZ and FW OTSGs. A detail description of the adopted procedure is available in Ref. [8]. The component sizing was inspired to the B&W layout and adapted considering: the thermo-dynamic constraints for PHTS and PCS water, unchanged from FP8 and contained in Refs. [1,2]; the latest available power source data for WCLL blanket and its distribution among BZ and FW PHTSs. They are collected in Table 1. In addition, the main design outcomes are summarized in Table 2.

3. Thermal-hydraulic analysis

3.1. Description of the thermal-hydraulic model

The RELAP5/MOD3.3 models for BZ and FW OTSGs were developed at DIAEE, revising and improving the ones adopted to perform transient analysis during previous activities, [10–12]. The same axial nodalization, reported in Fig. 2, was used for both components since they have the same thermal height. What differs between the two input decks are some parameters related to the OTSG transversal section (e.g., primary/secondary flow area, see Table 2).

Several aspects were carefully addressed while realizing the model. The *node-to-node ratio* is defined as the ratio between the length of two adjacent control volumes. This parameter reflects the nodalization homogeneity that reduces the possibility of numerical errors. For this, it was kept as uniform as possible (i.e., less than 1.25) throughout the overall mesh. The *slice nodalization technique* was also adopted. A vertical segmentation of the overall steam generator was performed based on selected quotes. They were chosen to keep the actual design elevations of the main internals. The axial mesh related to all the OTSG components (i.e., primary side tube bundle, secondary side lower downcomer, lower/upper riser and steam downcomer) was obtained respecting these reference heights. As a result, the same mesh length was used for the vertical control volumes belonging to different nodalization regions positioned at the same axial level. This technique improves the capability of the code to reproduce natural circulation. When adopted, fluid properties are evaluated at the same axial elevations for all the

Table 1
BZ and FW OTSG conceptual design: thermophysical data, [1,2].

System	Parameter	Unit	BZ	FW
PHTS	Power per OTSG	MW	581.5	379.0
	Blanket outlet Temperature	°C	328	328
	Blanket inlet Temperature	°C	295	295
	System pressure	MPa	15.5	15.5
	System Mass flow	kg/s	3010.6	1962.2
PCS	Feedwater inlet Temperature	°C	238	238
	Steam outlet Temperature	°C	300	300
	Steam outlet nozzle pressure	MPa	6.41	6.41
	Feedwater flow	kg/s	316.2	206.1

Table 2
BZ and FW OTSG conceptual design: geometrical data, [8].

Parameter	Unit	BZ	FW
Tube material	–	INCONEL 690	INCONEL 690
Tube N°	–	6943	4512
Tube OD[1]	mm	15.9	15.9
Tube thickness	mm	0.86	0.86
Tube p/D	–	1.4	1.4
Lattice	–	Triangular	Triangular
Shroud ID[1]	m	2.01	1.62
Shroud thickness	mm	25	25
Shroud OD	m	2.06	1.67
Shell ID	m	2.36	1.92
Shell thickness	mm	60	60
Shell OD	m	2.48	2.04
Thermal Length	m	12.98	12.98

[1] OD and ID stand for 'Outer Diameter' and 'Inner Diameter', respectively.

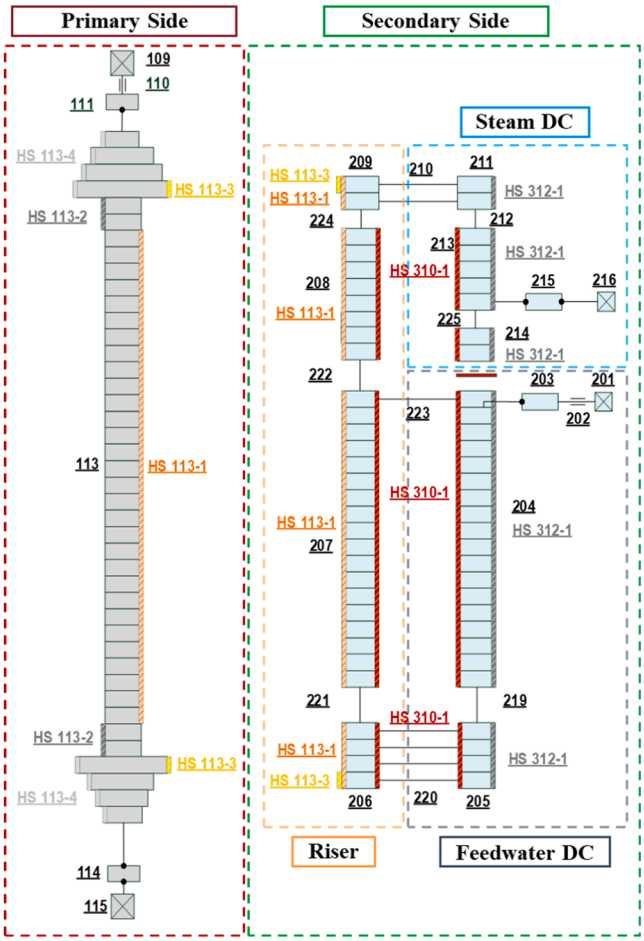

Fig. 2. RELAP5/MOD3.3 nodalization scheme for BZ and FW OTSGs.

nodalization regions, resulting in a proper evaluation of the natural circulation driving force and avoiding an error source on the simulation outcomes, [13]. Finally, the *fluid and material inventories* were rigorously maintained. In such a way, the component thermal inertia was simulated in the best possible manner.

The mesh characterizing the thermal height was selected considering the sensitivity discussed in § 3.1.1. Referring to the secondary side, most of the chosen vertical nodes were distributed among two ascendant pipes simulating the lower and upper riser sections (207 & 208 in Fig. 2). They are divided in correspondence of the recirculating window elevation. The same vertical nodalization was then used for the sequence of three descendant pipes modelling the series of steam downcomer, dead zone and lower downcomer (213, 214 & 204 in Fig. 2). It must be noted that the dead zone is a little annular region axially located between the steam outlet nozzles and the upper boundary of the lower downcomer. Here, fluid is stagnant. To properly model the lower and upper ports, the bottom and top parts of the downcomer and shroud volumes were simulated with dedicated pipe components (205, 206, 209 & 211 in Fig. 2) whose Control Volumes (CV) were connected by means of cross junctions (220 & 210 in Fig. 2). In addition, a further junction (223 in Fig. 2) was used to link the last CV of the lower riser with the first CV of the lower downcomer, modelling the Recirculating Window (RW).

The main concentrated pressure drops related to the secondary circuit are the ones associated with: feedwater inlet nozzles (branch 203 in Fig. 2), lower downcomer orifice plate (junction 219 in Fig. 2), lower ports, riser tube support plates (internal junctions of pipes 207 and 208), recirculating window, upper port and steam outlet nozzles (branch 215 in Fig. 2). They were all simulated by associating an equivalent K coefficient to the correspondent junction component (N.B. a branch component is a CV with included N junction components, up to nine). All the geometrical data needed to evaluate the K-coefficients were derived by the OTSG CAD model and thermomechanical design, widely described in Ref. [14]. Referring to the feedwater inlet and steam outlet nozzles, the related minor head losses were computed by using formulas for area contraction and expansion recommended in Idelchik hydraulic handbook, [15], and reported below.

$$\text{Area contraction: } K_{contraction} = 0.5 * \left(1 - \frac{A_{\min}}{A_{\max}}\right)$$

$$\text{Area expansion: } K_{expansion} = \left(1 - \frac{A_{\min}}{A_{\max}}\right)^2$$

The same expressions were also used for the lower and upper ports. The thirteen Tube Support Plates (TSP) selected for the OTSG conceptual design are equally spaced along the overall thermal height with a span conservatively assumed lower than one meter. The original B&W trefoil design was kept. It is extensively discussed in Ref. [16], where the broached hole flow area is indicated, as well as the correspondent K coefficient. The latter was evaluated by considering an ad-hoc empiric formula developed during a test campaign in a Framatome laboratory. Since the TSP design was maintained in the BZ and FW OTSGs, the computed value of the K-coefficient is also applicable. The presence of an orifice plate at the bottom of the lower downcomer is discussed in Ref. [17]. It is used to increase the stability in the recirculating loop, composed by the lower parts of downcomer and riser (up to the recirculating window). Within the cited study, this section of the OTSG was simulated with a RELAP5/Mod2 model. The K-coefficient associated with the orifice plate was assessed by best-fitting the pressure profiles obtained with the experimental data coming from the AREVA, Inc. Oconee Unit I nuclear power plant (South Carolina, USA). For the BZ and FW OTSGs, the orifice plate flow area was scaled from the B&W layout by using as scaling factor the ratio between the lower downcomer transversal sections. Hence, the K coefficient suggested in Ref. [17] for this component was still suitable for the current model. Finally, the RW consists in a circumferential cut of the shroud component. The ratio between the window height and the overall thermal height, as well as the component axial position, was derived from Ref. [16] and kept also for the BZ and FW OTSG layout. The total K-loss coefficient is the sum of the contributions due to the tube bundle crossing and the area change (contraction plus expansion, following the riser - aspirator port – lower downcomer flow path). For the first term, a recommended value is reported in Ref. [16] where it is computed by using the empirical correlation developed by AREVA for flow through staggered tubes. The others were computed with formulas provided in Idelchik hydraulic handbook, [15], and reported above.

Concerning the primary side, it was used a nodalization consistent with the one adopted for the secondary side (*slice nodalization technique*). The PHTS water flow path within the steam generator was simulated with a single equivalent pipe component, downwards oriented (113 in Fig. 2). The CV hydraulic features vary along the axial coordinate to properly model the series of components constituting the OTSG primary side, in particular: the upper head, the tube bundle and the lower head. Each head was simulated by means of four CVs. The head elevation change is equally distributed between them, and their flow areas were calculated to keep the head total water inventory. The tube bundle was modelled with CVs characterized by lumped parameters, in particular the total tube flow area and primary mass flow. Instead, the hydraulic diameter of the single tube was entered as input data. This modelling approach allows to keep the actual inventory and to properly model the bundle pressure drops. Two CVs were added at both bundle inlet and outlet to simulate the tube length inside the tubesheet thickness. The main concentrated pressure drops are related to the inlet/outlet nozzles and to the upper head/tube bundle and tube bundle/lower head interfaces. They are all area changes. Thus, the associated K-loss coefficients were evaluated with the formulas shown before. The primary inlet/outlet nozzle reference layout was derived from the OTSG CAD model [14].

RELAP5 Heat Structure (HS) components were used to simulate the thermal transfer taking place inside the steam generators, as well as the component heat losses. Furthermore, they allow to account for the OTSG steel inventory (i.e., thermal inertia). The thermal coupling between primary and secondary sides was modelled with two heat structures. The former was used to simulate the heat transfer across the tube bundle (HS 113-1, orange in Fig. 2), while the latter the thermal exchange through the tubesheets (HS 113-3, yellow in Fig. 2). An additional heat structure (HS 310-1, red in Fig. 2) allows the exchange of power within the secondary side, i.e., between the lower/steam downcomer and the riser across the shroud thickness. The component heat losses were accounted by means of two heat structures. The first related to the lower and upper head (113-4, light gray in Fig. 2), the second referring to the steam generator vessel (312-1, dark grey in Fig. 2). As external boundary conditions, it was considered a constant containment temperature (30 °C), and a constant Heat Transfer Coefficient (HTC, 8 W/m^{2}K). Ten centimeter of thermal insulation was applied to the OTSG external surface.

For the solid materials involved in the heat transfer problem, RELAP5 code prompts the user to enter the needed thermal properties. The required input consists of two tables collecting the thermal conductivity and heat capacity trends against temperature, [18]. These properties were used to solve the Fourier's law for heat conduction in solid layers, [19]. Selected tube material is INCONEL 690, due to its improved corrosion and erosion resistance. For the steam generator internals and vessel, the chosen steels were derived from the thermomechanical design, [14]. The thermal properties for all these structural materials were taken from the ASME code, [20]. Regarding the insulator, an example of suitable material for OTSG application is reported in Ref. [21] together with its thermal properties, preliminary used for calculation purposes.

3.1.1. Mesh sensitivity

Firstly, a sensitivity analysis was carried out to investigate the

influence of the thermal height nodalization on the calculation results. The aim was to select the minimum number of nodes providing acceptable results, testing at the same time the model stability. The overall tube length, reported in Table 2, was divided into different numbers of axial nodes, always respecting the slice nodalization technique, i.e., adopting the same vertical mesh for both primary and secondary sides. The cases considered are summarized in Table 3. The sensitivity focused on the pipes simulating the lower/steam downcomer and the lower/upper riser, while the components modeling the lower/upper ports were excluded. The cases were labeled with the format *'n-n'* (or a multiple), where the first *n* refers to the mesh number in the OTSG lower section (up to the recirculating window), while the second *n* corresponds to the vertical nodes belonging to the OTSG upper part (from the recirculating window up to the upper tubesheet). Since the axial nodalization is the same, the simulations were performed considering the BZ OTSG at BoL conditions.

Some of the OTSG data reported in Table 1 were implemented in the model as boundary conditions. Referring to the secondary (PCS) side, the steam line pressure and the feedwater inlet temperature were set by means of two time-dependent volumes (201 and 216 in Fig. 2). Regarding the primary (PHTS) side, the outlet pressure, the inlet temperature and the inlet mass flow were imposed by means of two time-dependent volumes (109 and 115 in Fig. 2) and a time-dependent junction component (110 in Fig. 2), respectively. In addition, a Proportional-Integral (PI) controller was associated with the time-dependent junction setting the inlet feedwater mass flow (202 in Fig. 2). By tuning the latter, the control system regulates the heat transfer within the steam generator to obtain the required temperature at the primary side outlet (i.e., BB inlet, see Table 1). For this, among the OTSG global parameters, the most interesting for the sensitivity purpose are the feedwater mass flow and the steam outlet temperature, shown in Fig. 3a and 3b, respectively. What is investigated is whether the steam generator simulated heat transfer capabilities depend on the nodalization adopted. If not, the feedwater mass flow obtained from the PI regulation should be the same for all the cases considered, as well as the steam outlet temperature resulting from the power balance performed at the secondary side. Although, as visible from the results contained in Fig. 3, increasing the mesh number from *'n-n'* to *'2n-2n'* produces a significant variation in the selected figures of merit. Instead, for smaller meshes (higher mesh number, case *'3n-3n'*) the results are nearly unaltered. In addition, what is worth to be noted is that rising the node number in the OTSG lower section (case *'3n-n'*) has a deeper impact on the calculation results than increasing them in the upper part (case *'n-3n'*). Considering the simulation outcomes, the axial nodalization related to case *'2n-2n'* was selected as reference for the following analysis.

3.2. Operations at full plasma power state

The RELAP5 model discussed above was used to preliminary evaluate the OTSG thermal-hydraulic behavior during full plasma power state (also named pulse) of DEMO normal operations. The input deck was tested to demonstrate the compliance of its predicted performances with the design specifications, reported in Ref. [8]. Both BoL and EoL conditions were selected to be simulated. At EoL, some modifications were performed on the tube bundle heat structure (113-1 in Fig. 2) to model the tube plugging and fouling. The former was accounted by reducing the heat transfer area. Concerning the fouling, only secondary side thermal resistance was considered. Such additional term was simulated by adding an equivalent layer of deposit to the heat structure overall thickness. The adopted values for tube plugging and fouling were derived from Ref. [8]. They are reported in Table 4.

For a heat exchanger, standard verification procedure foresees that primary and secondary inlet conditions are imposed and the thermal power exchanged is checked. This procedure cannot be applied in the current simulation activity. In fact, during DEMO pulse, blanket power and inlet/outlet temperatures (so also the mass flow) are strict requirements. For this, in the calculations performed, primary side inlet conditions are set while the PHTS water outlet temperature is monitored by the PI controller acting on the OTSG secondary flow (see § 3.1). Being all the primary side parameters set or controlled, also the steam generator exchanged power is imposed. On the secondary side, feedwater inlet temperature is a boundary condition since it depends on the feedwater preheaters train installed in the PCS upstream the OTSG. In addition, steam line pressure is also imposed.

Simulations were performed considering both BZ and FW OTSGs. Although, it is important to remind that both steam generators were scaled from the same reference layout (B&W) and the same scaling procedure was adopted (see Ref. [8]). Thus, a similar, if not the same, thermal-hydraulic behavior was expected from them. This was confirmed by numerical outcomes. Indeed, all the intensive parameters (e.g., pressures, temperatures and collapsed levels) are practically the same for both BZ and FW OTSGs. Only extensive parameters (e.g., mass flows and mass inventories) vary accordingly with the different power level associated to each steam generator. For this and for sake of clarity, only the results related to the BZ OTSG are collected in Table 4 and in the figures present in this section.

Referring to Table 4, the parameters indicated with '**(BC)**' are the ones set as boundary conditions. Moreover, the indicated values for primary and secondary side pressure drops were evaluated by using the Bernoulli equation:

$$\Delta p_{Drops} = (p_1 - p_2) + g * (\rho_1 h_1 - \rho_2 h_2) + 0.5 * \left(\rho_1 v_1^2 - \rho_2 v_2^2\right)$$

where, the subscripts 1 and 2 refer to inlet and outlet sections, respectively. Regarding the secondary side, the major contribution to the overall pressure drops is associated with the feedwater inlet nozzles. Indeed, they are equipped with holes through which feedwater is sprayed down into the annular heating chamber, see § 2 and Fig. 1c. Hole dimensions are very low to reduce the feedwater droplet size and enhance the mixture with the steam coming from the bundle region. Although, the pressure drops related to this equipment are significant. This is witnessed by the pressure values reported in Fig. 4, related to some relevant points belonging to the OTSG secondary side, and by the quite uniform pressure field contour visible in Fig. 5a. What is important to be pointed out is that, when an open circuit was simulated, as in the case of OTSG primary and secondary sides, RELAP5/MOD3.3 sets the reference system pressure at the outlet time-dependent volume (reminding that it also imposes the inlet mass flow rate). From there, it computes the pressure profile up to the inlet time-dependent volume by taking into account the static head and the pressure drops along the fluid

Table 3
Sensitivity on thermal height mesh number: selected cases.

Case	Mesh Number [-]				Mesh Size [m]			
	Lower Ports	Up to RW	From RW	Upper Port	Lower Ports	Up to RW	From RW	Upper Port
'n-n'	4	20	10	2	0.185	0.396	0.396	0.185
'n-3n'		20	26			0.396	0.15	
'2n-2n'		39	19			0.205	0.205	
'3n-n'		53	10			0.15	0.396	
'3n-3n'		53	26			0.15	0.15	

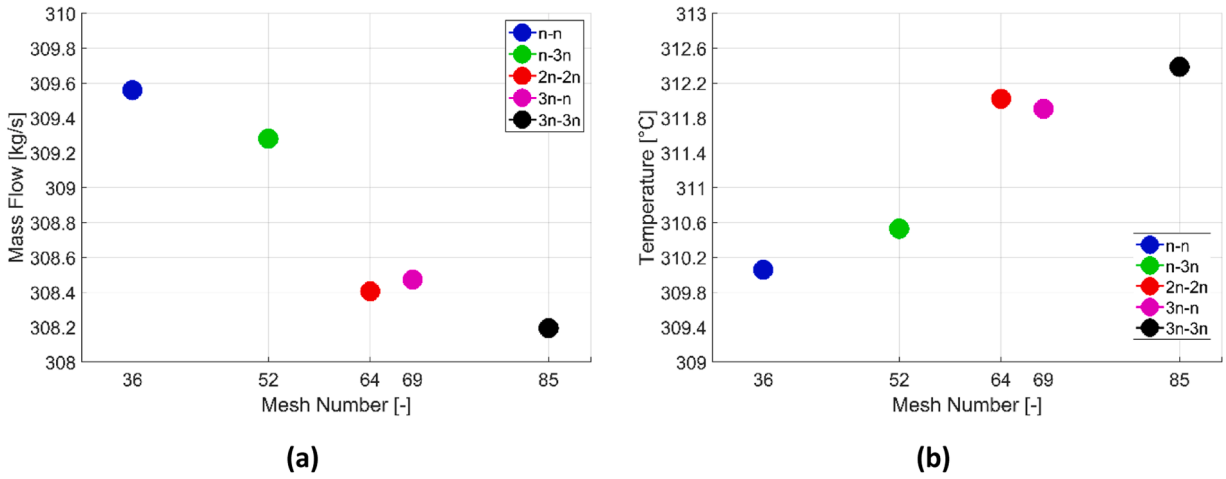

Fig. 3. Sensitivity on thermal height mesh number: feedwater mass flow (a), steam outlet temperature (b).

Table 4
Full plasma power state: main results related to BZ OTSG.

Parameter	Unit	EoL	BoL
DESIGN DATA			
Secondary fouling resistance	m^2K/W	2.10E-05	0.00E-00
Tube bundle plugging	%	2.5	0
POWER BALANCE			
Exchanged power	MW	581.5	581.5
Heat losses	kW	16.3	16.3
TEMPERATURES			
Primary side inlet **(BC)**	°C	328	328
Primary side outlet	°C	295	295
Secondary side inlet **(BC)**	°C	238	238
Secondary side outlet	°C	300	312
PRESSURES			
Primary side outlet **(BC)**	MPa	15.5	15.5
Secondary side outlet **(BC)**	MPa	6.41	6.41
MASS FLOW RATES			
Primary side **(BC)**	kg/s	3010.6	3010.6
Secondary side Feedwater	kg/s	316.2	308.4
Secondary side Recirculating	kg/s	43.4	38.6
COLLAPSED LEVELS			
Riser	m	2.34	1.92
Downcomer	m	4.29	4.04
MASS INVENTORY			
Primary Side	kg	13,580	13,777
Secondary Side	kg	7254	6542
PRESSURE DROPS			
Primary Side	kPa	145.0	141.6
Secondary Side	kPa	175.1	168.9

flow path. For this, in Table 4, the primary and secondary side system pressures, that are boundary conditions, are referred to the outlet. In particular, for the secondary side, this is consistent with the PCS requirement in Ref. [1,2], where the system pressure is considered at the steam outlet nozzle.

Other relevant OTSG parameters are collected in Fig. 5b, referring to secondary side thermodynamic quality contour, and Fig. 6a and b, related to temperature and HTC axial profiles. Starting from the shroud bottom, as feedwater is converted to superheated steam, three heat transfer regions can be identified in the steam generator secondary side. The first one is the Nucleate Boiling Region (NBR), where saturated feedwater begins to boil. Tube outer surface remains wetted while small bubbles rapidly form and break away from it. Thanks to the turbulence due to bubble formation, this heat transfer mode ensures a high heat transfer coefficient. Most of the primary-to-secondary thermal exchange occurs in the NBR. Thus, its extension is roughly proportional to the OTSG power. The nucleate and forced convective boiling continue until enough water is vaporized and the liquid layer is replaced by steam on the tube outer surface. Therefore, Film Boiling Region (FBR) occurs at high qualities after the dry-out point and fully develops within a very short axial distance. In the film boiling heat transfer, the heat flux is sharply reduced, and heat transfer occurs by convection through the steam and evaporation of entrained liquid droplets in the saturated core. At FBR top, only dry steam is present. Finally, in the SuperHeating Region (SHR), thermal power transferred from primary fluid is used to produce superheated steam. Thermal exchange is characterized by low secondary side heat transfer coefficient.

What is worth to be emphasized is that dry-out occurs nearly at 60% of the overall thermal height. This can be detected by looking at the axial quote where HTC drops in Fig. 6b. Therefore, the recirculating flow is almost dry steam. This matches the recommendations present in Refs. [5–7] about the good practices in the OTSG operation. As expected, the majority of the heat exchange takes place in the first part of the thermal height, i.e. in the NBR (see Fig. 6b). When dry-out occurs, the secondary side resistance becomes the prevalent one, significantly reducing the thermal exchange. This is also detectable in the slope change related to the primary side temperature (see red line in Fig. 6a).

Between EoL and BoL the main difference is the reduction of the NBR extent, i.e., the anticipation, axially speaking, of the dry-out occurrence. This effect can be detected in Fig. 6b by comparing blue (EoL) and red (BoL) lines. It is due to the increased heat transfer efficiency at BoL, caused by the higher heat transfer area and the lack of the deposit thermal resistance. Such higher heat transfer efficiency allows to obtain dry steam at lower axial quote (with respect to EoL) and so to exit from the steam generator with a higher outlet temperature (compare the parameter values in Table 4). The lowering of the dry-out quote also reduces the riser collapsed level. Being the OTSG power imposed, the increase in the steam outlet temperature is compensated by a slight decrease in the feedwater mass flow. This also diminishes the secondary side pressure drops. Thus, in the recirculating loop, the equilibrium is reached with a lower level in the heating chamber. Indeed, the driving force due to the column density difference must counterbalance reduced pressure drops. Also, the steam aspirated from the bundle region (i.e., recirculating mass flow) is accordingly lower.

3.3. *Sensitivity on selected design parameters*

Some scoping calculations were performed in order to evaluate the influence on the OTSG performances of some selected design parameters. In particular, the orifice plate and recirculating window flow areas were chosen. For these components, the function, as well as the reference design and modelling, was discussed in § 2 and 3.1 and briefly recalled in the following. New simulations were run varying one of the two parameters while keeping the other constant (and equals to its

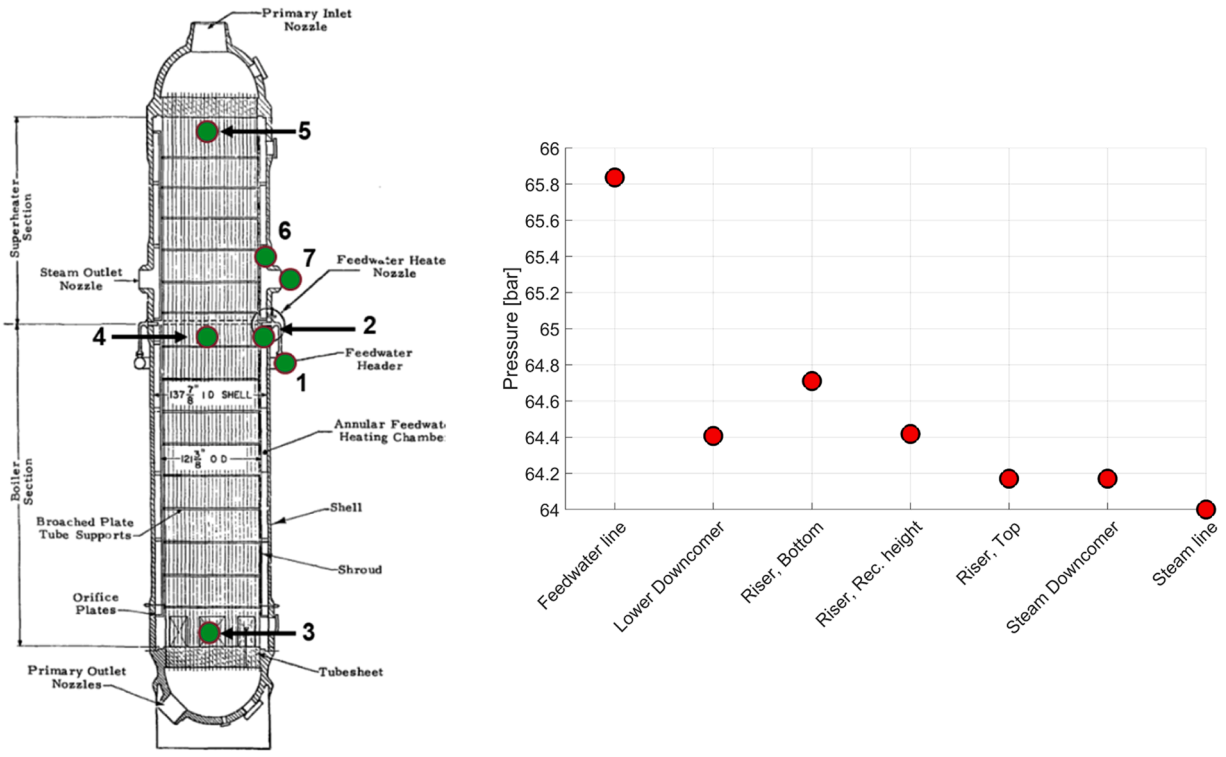

Fig. 4. Full plasma power state: pressure in relevant points belonging to BZ OTSG secondary side (EOL).

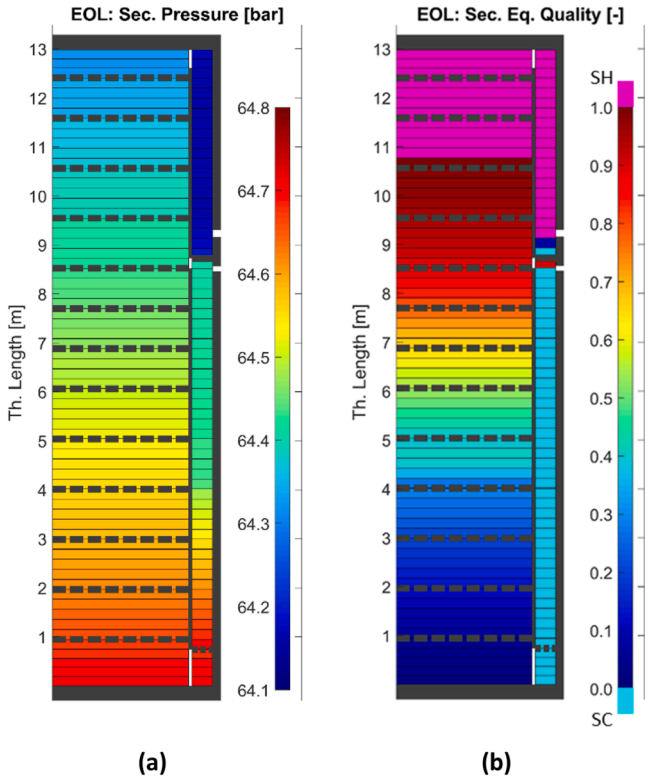

Fig. 5. Full plasma power state: BZ OTSG secondary side pressure (a) and thermodynamic quality (b) contours (EOL).

reference value).

Referring to the orifice plate, it is located at the bottom of the lower downcomer just above the lower ports connecting the component to the central riser. Its main function is increasing the stability of the recirculating loop, composed by the feedwater annular heating chamber and the lower section of the bundle region (up to the recirculating window). For the BZ and FW OTSGs, the reference value for the orifice plate flow area was scaled from the original B&W layout, described in Ref. [17]. It is evidenced with a blue marker in Fig. 7. It corresponds to nearly 14% of the lower downcomer flow area. A sensitivity was carried out on this parameter, by both increasing and decreasing its value. Boundary conditions applied to the calculations are the same already described in § 3.2,as well as the control system acting on the feedwater flow. System code results evidenced some interesting aspects. First, what is worth to be noted is that varying the orifice plate flow area mainly influences the behavior of the recirculating loop, while the OTSG global parameters (e.g., feedwater flow and steam outlet temperature) remain substantially unchanged. The main effect provoked by the decrease of the orifice plate flow area is the increase of the pressure drops in the recirculating loop. This causes a rise of the downcomer level required to provide the needed gravity head, as visible in Fig. 7a. Moreover, the new equilibrium between gravity head and pressure drops is reached in correspondence of a lower recirculating mass flow, see Fig. 7b. The opposite occurs when orifice plate flow area is increased. Even if not included in Fig. 7, other analyses were conducted either further decreasing the orifice plate flow area or eliminating the component from the model. In the first case, what was observed looking at the simulation results is that exists a threshold value for the orifice plate flow area below which the incoming feedwater flow bypasses the recirculating loop (annular heating chamber plus bundle region lower section) and passing through the recirculating window goes directly to the upper part of the bundle region, completely altering the OTSG operations. Instead, in case the component is eliminated, oscillations appear in the calculation results, not only for the quantities referred to the recirculating loop but also for the OTSG global parameters. This confirms the important role played by the orifice plate in stabilizing the steam generator operations.

For what concerns the recirculating window flow area, also this parameter was scaled by B&W layout, available in Ref. [16]. The sizing procedure was already described in § 3.1. The reference value is

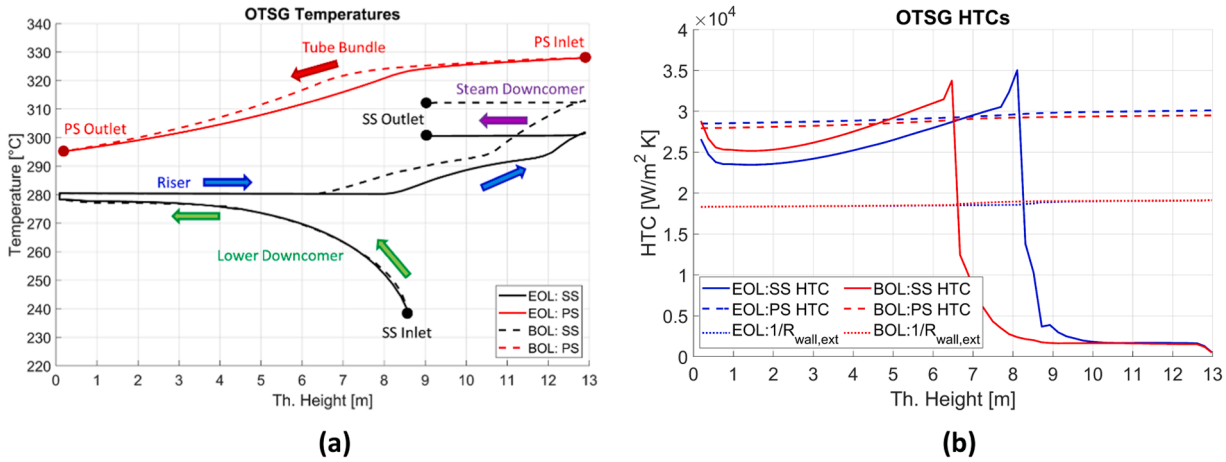

Fig. 6. Full plasma power state: BZ OTSG temperature (a) and HTC (b) profiles (EOL).

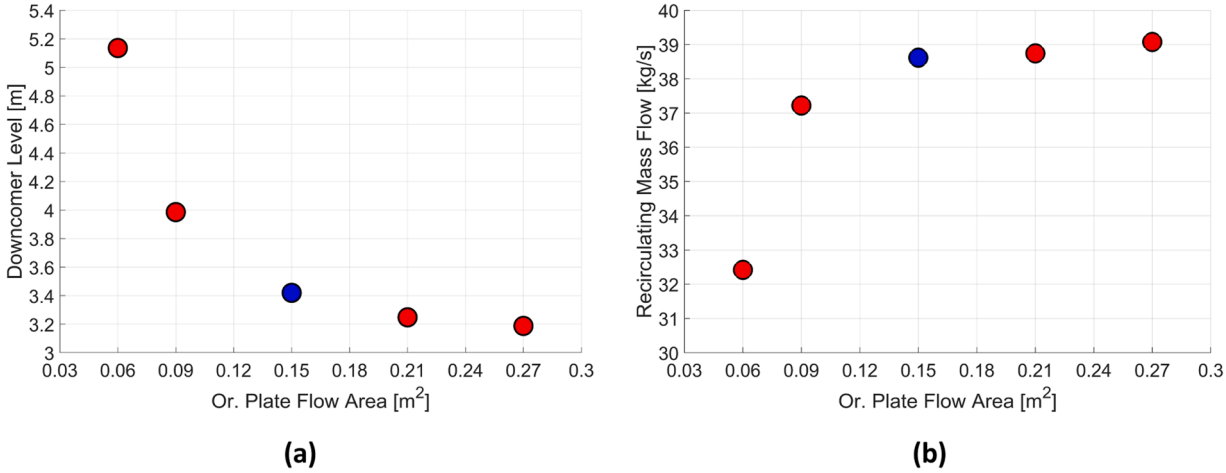

Fig. 7. Sensitivity on orifice plate flow area: BZ OTSG secondary side downcomer level (a), and recirculating mass flow (b).

highlighted by a blue marker in Fig. 8. Even in this case, a sensitivity was performed by varying this parameter. The boundary conditions and control system so far adopted for calculation purposes were kept also for these new simulations. Numerical results evidenced that this parameter acts in a similar way with respect to orifice plate flow area. Its influence is mainly related to the recirculating loop, without significant alteration of the OTSG global operations. Recirculating window represents another minor head loss belonging to the recirculating loop, just like the orifice plate. Decreasing its flow area, increase the overall pressure drops in the circuit and provokes a correspondent rise of the downcomer level, see Fig. 8a. What is worth to be noted is that for low values of RW flow area the downcomer level variation is significant, while for greater values the

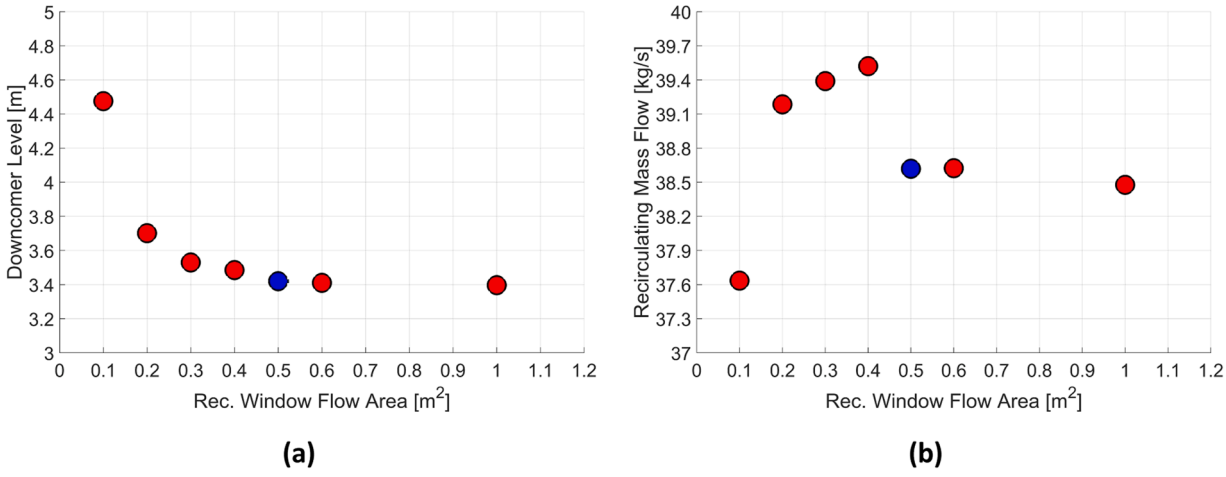

Fig. 8. Sensitivity on recirculating window flow area: BZ OTSG secondary side downcomer level (a), and recirculating mass flow (b).

effect on this parameter is practically null. This is due to the fact that the concentrated pressure drop associated with the recirculating window becomes negligible with respect to the one related to the orifice plate. The reference value, scaled from B&W layout, belongs to saturated part of the trend in Fig. 8a. This means that, in the reference design, analyzed in § 3.2, the orifice plate is the dominant pressure drop in the recirculating loop, as recommended in Refs. [5–7] for a proper operation of the OTSG component. Finally, only a weak influence of the recirculating window flow area on the recirculating mass flow can be detected, see Fig. 8b. For low values, the trend is like the one observable in Fig. 7b. For higher values, a small step down can be detected, after which the recirculating flow value stabilizes.

The sensitivity results highlight the effectiveness of the adopted values for the RW and orifice plate flow areas. This is an expected outcome since they were scaled by the B&W original design. Although, the OTSG thermal-hydraulic performances will be furtherly studied in the next years by including a complete characterization of these pressure drops at different power levels (i.e., feedwater mass flows). It is not excluded that these future studies will lead to a refinement of the RW and orifice plate layouts. Eventually, these components can also be investigated in detail by using three-dimensional CFD calculations: Finally, they will be characterized with dedicated tests of the experimental campaign that will be performed on the OTSG component (see the conclusion section).

3.4. Operations at reduced power levels

Finally, the OTSG thermal-hydraulic performances were also investigated at reduced power levels. DEMO normal operations foresee a pulsed plasma regime alternating two hours of full plasma power state with ten minutes of dwell time. Therefore, also the OTSGs installed in the BB PHTSs experience time-dependent operations with periodic switches from full load to low load conditions and vice versa.

The RELAP5 input deck described in § 3.1 and used for the simulation activity discussed so far is a standalone model of the BZ and FW OTSGs. It does not consider the rest of the PHTS circuit, including both the sections within and outside the vacuum vessel. Above all, it does not take into account the thermal inertia of the corresponding blanket subsystems, namely the BZ and the FW. As demonstrated by previous studies referring to the pulse-dwell-pulse transitions, [10], the breeding blanket plays a fundamental role in influencing the thermal field in the related PHTSs. For this, the current OTSG standalone model is not appropriate for a proper evaluation of the component transient behavior during the pulsed plasma regime characterizing the DEMO normal operations. In addition, it must be considered that the BZ thermal inertia is much higher than the FW one due to the large lead-lithium inventory. Hence, during this operative scenario, the thermal-hydraulic boundary conditions for the BZ and FW OTSGs are very different, deserving separate calculations to accurately assess them both. Even if the actual power transitions cannot be simulated with the current model, the input deck can still be used to preliminary characterize the component thermal-hydraulic behavior within the entire power range expected for it. The latter swings from 100% to 1% of rated value (reported in Table 1). Indeed, the decay heat produced in the DEMO WCLL blanket during dwell time is estimated to be the 1% of the plasma power during pulse. For this analysis, since the focus is only on the steam generator, without the influence of the downward system, only the BZ OTSG is considered. The corresponding FW PHTS component has the same performances, for the reasons discussed in § 3.2.

Thus, a transient analysis was performed by reducing the BZ OTSG power level in EOL conditions. Steam generator power was decreased in a stepwise mode with stages of 10% lasting for 1000 s, from 100% to 10% of rated value. In addition, 5%, 2% and 1% steps were considered. In the calculation, power reduction was simulated by imposing the OTSG primary side inlet temperature as a stepwise boundary condition. Instead, primary mass flow was kept constant. At the secondary side, feedwater inlet temperature was maintained. Moreover, two different control systems for feedwater flow were tested: the former controls the primary system minimum temperature (labeled 'keep T_{min}' and characterized by blue trends in the figures of this section), while the latter the primary system average temperature (labeled 'keep T_{ave}' and characterized by red trends in the figures of this section). The primary system average temperature was preliminary considered as the mean between OTSG inlet and outlet. The system code results related to the main steam generator parameters are collected in Fig. 9.

Calculation outcomes evidenced a direct correlation between OTSG power level and secondary side feedwater flow and riser collapsed level. This is an important feedback obtained by the transient analysis. In the simulations performed, steam generator power is imposed and gradually decreased by means of a proper choice of primary side water inlet thermodynamic conditions (see discussion above and Fig. 9a and c). To follow the load reduction, the control system decreases the feedwater flow (Fig. 9d) provoking the NBR withdrawal at the OTSG secondary side (Fig. 10a and b). In such a way, the dry-out is anticipated and the secondary side HTC drops, becoming the prevalent thermal resistance and heavily penalizing the heat transfer. The water liquid content within the bundle region, represented by the riser collapsed level, is strongly related to the NBR extent. A reduction of the latter causes a proportional diminution of the former (blue and red solid lines in Fig. 9f). The direct correlation between bundle region water liquid content, NBR extent and overall HTC makes the riser collapsed level the most effective figure of merit to represent the exchanged power within the OTSG. Moreover, calculation outcomes show that varying the secondary side feedwater flow is an efficient way to change the steam generator load (with the hypothesis of keeping the primary side water thermodynamic conditions unmodified).

Comparing the two control systems, what can be detected is that the former (keep T_{min}, Fig. 10a) is characterized by higher dry-out quotes with respect to the latter (keep T_{ave}, Fig. 10b). This is due to lower temperature differences between steam generator primary and secondary sides. When minimum temperature is kept at the primary system, power reduction leads to a lowering of OTSG inlet (maximum) temperature that step by step approaches the outlet (minimum) one (see Fig. 9a). The system average temperature follows the same trend, starting from nominal value, that is the one maintained in the other control strategy, and dropping down to the primary minimum temperature. This decreases the available temperature difference between steam generator primary and secondary sides. Consequently, also the heat exchange efficiency in the NBR is reduced, leading to its higher axial extensions (in Fig. 10a w.r.t. Fig. 10b). Moreover, the dry-out anticipation occurring with decreasing power leads to an extension of the SHR. Accordingly, the steam outlet temperature rises approaching the primary inlet one. For the reasons just discussed, in Fig. 9b the trend related to first control system (blue, keep T_{min}) lies below the one of the second control system (red, keep T_{ave}).

What can be detected by looking at Fig. 9 is the presence of some oscillations in the numerical results occurring for intermediate power levels (30–50%). They are mainly related to the case where primary average temperature is kept. However, it is important to note that both control systems ensure stable OTSG operations at the rated value (pulse), as well as for very low power levels (dwell time). These are the only two states where OTSG is required to operate steadily or quasi-steadily during DEMO normal operations. Indeed, the steam generators experience intermediate power levels only for very brief time windows during pulse-dwell and dwell-pulse transitions. In this perspective, numerical results suggest that the first control concept enables the steam generator to operate in a more stable way along the entire power range considered.

Another interesting feature to be underlined is that, under a certain power threshold, both riser and downcomer collapsed levels drop below the top quote of the water ports located at the component bottom (see Fig. 9f). The decrease of downcomer level follows the reduction of

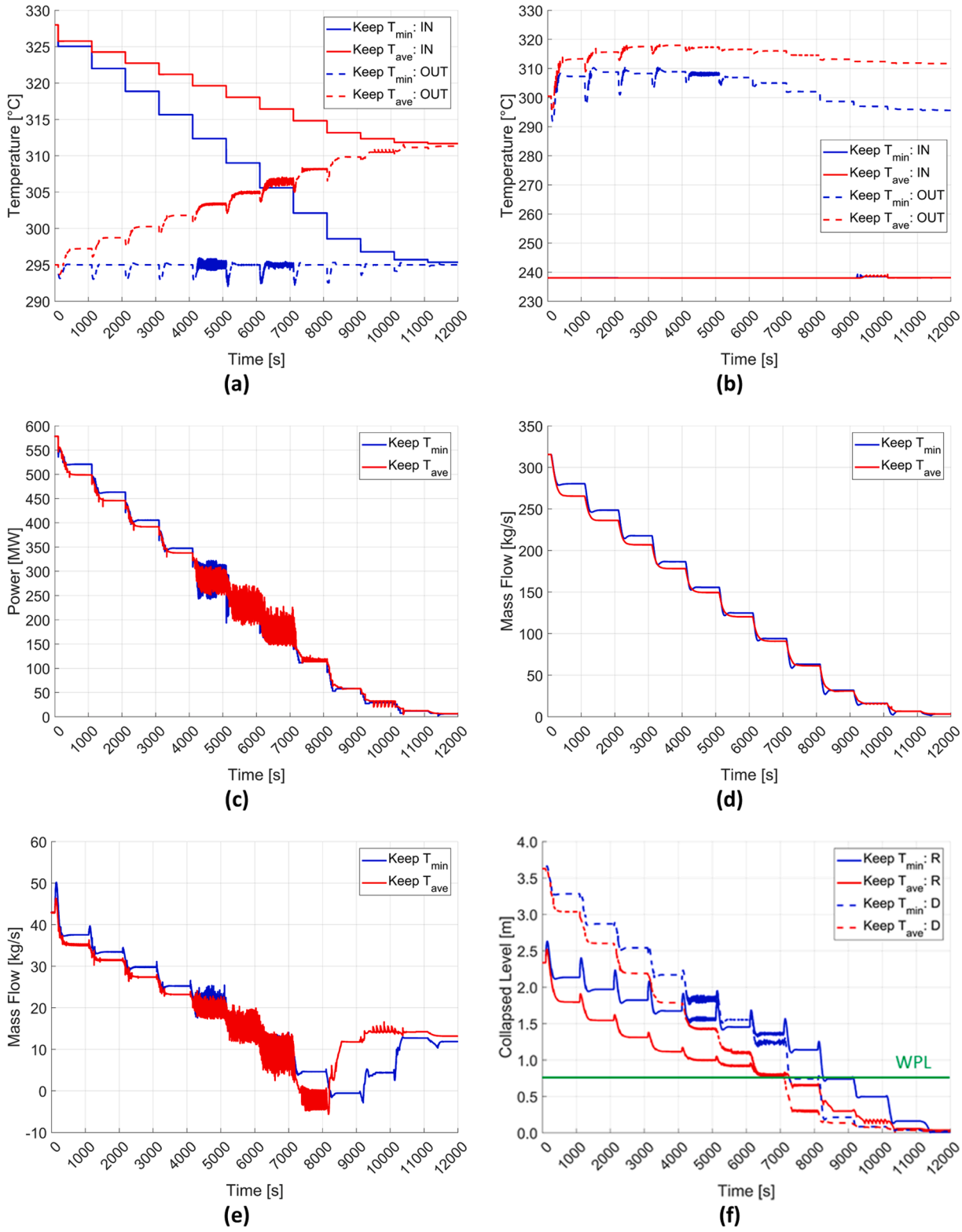

Fig. 9. BZ OTSG operations at reduced power levels: primary (a) and secondary (b) side temperatures; exchanged power (c); secondary side feedwater (d) and recirculating (e) mass flows; secondary side riser and downcomer levels (f).

feedwater flow. Indeed, the pressure drops in the recirculating loop diminish and consequently require a lower downcomer level to achieve the needed gravity head. For BZ and FW OTSGs the lower port axial height was scaled from B&W layout by considering the ratio between thermal heights. The reference value was derived from Ref. [17]. Water Ports Level (WPL) is represented by the green horizontal line in Fig. 9f.

A final aspect to be highlighted is the trend characterizing the recirculating flow (Fig. 9e). With decreasing power, this parameter reduces accordingly to the lowering of the main feedwater flow. Although, when water ports at the component bottom are uncovered, it rises again settling to a nearly constant value. This occurs since two parallel flows develop in the recirculating loop: the feedwater flow and a separated

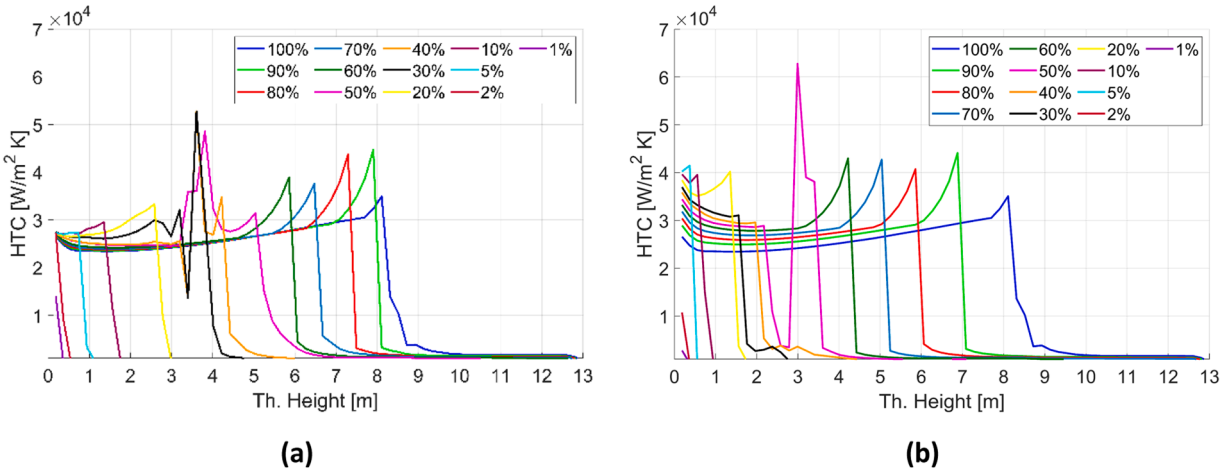

Fig. 10. BZ OTSG operations at reduced power levels: secondary side HTC axial profile at different power levels in case control system keeps the primary system minimum(a) and average (b) temperature.

steam flow. In the annular heating chamber, the former is characterized by liquid droplets that are heated to saturated conditions by the steam phase. In fact, the code predicts vertical annular mist flow in this zone. Liquid droplets fall by gravity in the water sump located just above the lower tubesheet, whose level is reducing according to the power exchanged (and it is lower than the top quote of the water ports). There, water quickly vaporizes up to superheated conditions (see lower dry-out quotes shown in Fig. 10a and b) becoming a contribute to the overall steam flow characterizing the shroud region. Indeed, for this zone, system code predicts mist flow regime. In addition, a second steam flow recirculates in the lower part of the steam generator driven by the difference of steam temperature between lower downcomer (where steam is cooled by liquid droplets) and lower riser (where steam is heated by primary coolant). In the annular heating chamber, it constitutes the steam core of the annular mist flow (slower than the liquid droplets that are heavier). Then, it flows through the upper part of the water ports, that is uncovered. In fact, horizontal stratified regime is predicted. Finally, it contributes to the overall steam stream flowing along the lower part of the riser, up to the recirculating junction. Since driven only by the steam temperature difference, the magnitude of this steam flow remains almost unaltered with the decreasing power level. However, this is only a preliminary explanation of the recirculating mass flow trend and further investigations related to this aspect are still needed. In fact, they are planned developments of the activity.

4. Conclusions

Within the framework of FP9 WPBoP activities DIAEE of Sapienza University of Rome developed the thermal-hydraulic conceptual design of the OTSGs to be installed in the DEMO WCLL breeding blanket primary cooling circuits. The present paper dealt with the presentation of the analyses performed on such components. To fulfill this scope, a complete model of the steam generator was prepared by using the best-estimate system code RELAP5/MOD3.3.

Firstly, the input deck was used to study the OTSG behavior during full plasma power state, considering both BoL and EoL conditions. Constant boundary conditions were applied to: primary/secondary inlet temperature and outlet pressure and primary mass flow. A control system was associated to the feedwater flow to tune the heat transfer within the steam generator and obtain the required primary outlet temperature. Thus, the OTSG exchanged power was imposed. These features are common to all the calculations discussed in this paper, if not specified otherwise. Results evidenced that BZ and FW components have the same performances (i.e., same intensive parameters), as expected since they were scaled by the same reference layout (B&W). Most of the heat exchange occurs before the dry-out occurrence, thus in the NBR. After, the secondary side HTC drops, significantly reducing the thermal exchange. For this, the secondary side HTC profile is a quite effective figure of merit to represent the steam generator performances. At BOL, the higher heat transfer efficiency allows to obtain dry steam at lower axial quote (with respect to EOL) and so to exit from the steam generator with a higher outlet temperature. Being the steam generator power imposed, the increase in the steam outlet temperature is compensated by a slight decrease in the feedwater mass flow (regulated by the control system).

After, sensitivity studies were conducted on some selected design parameters, namely the orifice plate and recirculating window flow areas. New simulations were run varying one of the two parameters while keeping the other constant (and equals to its reference value). Numerical outcomes highlighted that their influence is mainly related to the recirculating loop, without significant alteration of the OTSG global parameters (e.g., feedwater flow, steam outlet temperature). They are both concentrated pressure drops belonging to the recirculating loop. Thus, when flow areas are decreased the downcomer level rises to provide the needed gravity head. In the reference design, the dominant pressure drop is the orifice plate, as recommended by the good practices about the OTSG operations.

Finally, the OTSG thermal-hydraulic behavior was investigated also at reduced power levels. This is a crucial aspect of the component design. Indeed, BB OTSGs experience alternated phases of full-load and low-load because of the pulsed nature of the plasma regime characterizing the DEMO normal operations. Steam generator power was decreased in a stepwise mode from 100% (pulse phase) to 1% (dwell time). In the calculations, power reduction was simulated by imposing the OTSG primary side inlet temperature as a stepwise boundary condition. The other boundary conditions were unchanged. Although, at the secondary side, two different control systems for feedwater flow were tested, controlling the primary system minimum and average temperatures, respectively.

Calculation outcomes evidenced a direct correlation between OTSG power level and secondary side feedwater flow and riser collapsed level. Indeed, to follow the load reduction, the control system decreases the feedwater flow provoking the NBR withdrawal (dry-out anticipation) at the OTSG secondary side. This causes a diminution of the secondary (and thus overall) HTC, penalizing the heat transfer. Moreover, the water liquid content within the bundle region, represented by the riser collapsed level, lowers accordingly with the reduction of the NBR extent. The direct correlation between bundle region water liquid content, NBR extent and overall HTC makes the riser collapsed level the most effective figure of merit to represent the exchanged power within the OTSG.

Moreover, calculation outcomes show that varying the secondary side feedwater flow is an efficient way to change the steam generator load (with the hypothesis of keeping the primary side water thermodynamic conditions unmodified).

For both control systems, some oscillations in the numerical results occur for intermediate power levels (30–50%). They are mainly related to the case where primary average temperature is kept. However, it is important to note that both control strategies ensure stable component operations at the rated value (pulse), as well as for very low power levels (dwell time). These are the only two states where OTSG is required to operate steadily or quasi-steadily during DEMO normal operations. Indeed, the steam generators experience intermediate power levels only for very brief time windows during pulse-dwell and dwell-pulse transitions. In this perspective, numerical results suggest that the first control concept (keeping the primary system minimum temperature) enables the steam generator to operate in a more stable way along the entire power range considered.

A final aspect to be highlighted is that, under a certain power threshold, both riser and downcomer collapsed levels drop below the top quote of the water ports located at the component bottom. When this occurs, the recirculating flow, so far decreasing with the feedwater flow, rises again settling to a nearly constant value. This occurs since two parallel flows develop in the recirculating loop: the feedwater flow and a separated steam flow. Although, this is only a preliminary explanation of the recirculating mass flow trend and further investigations related to this aspect are still needed. In fact, they are planned developments of the activity.

All the analyses presented in this paper will be furtherly refined during the next years of FP9 activities. Moreover, the OTSG operations will be fully tested in the STEAM facility that will be held in the ENEA research center of Brasimone. It will host a full height mockup of the BB OTSG, [22]. The test campaign will provide all the experimental data needed to validate the system code results discussed in this paper.

Declaration of Competing Interest

The authors declare that they have no known competing financial interests or personal relationships that could have appeared to influence the work reported in this paper.

Data availability

No data was used for the research described in the article.

Acknowledgments

This work has been carried out within the framework of the EUROfusion Consortium, funded by the European Union *via* the Euratom Research and Training Programme (Grant Agreement No 101052200 — EUROfusion). Views and opinions expressed are however those of the author(s) only and do not necessarily reflect those of the European Union or the European Commission. Neither the European Union nor the European Commission can be held responsible for them.

References

[1] L. Barucca, et al., Maturation of critical technologies for the DEMO balance of plant systems, Fusion Eng. Des. 179 (2022), 113096, https://doi.org/10.1016/j.fusengdes.2022.113096.
[2] I. Moscato, et al., Tokamak cooling systems and power conversion system options, Fusion Eng. Des. 178 (2022), 113093, https://doi.org/10.1016/j.fusengdes.2022.113093.
[3] A. Del Nevo, et al., Recent progress in developing a feasible and integrated conceptual design of the WCLL BB in EUROfusion project, Fusion Eng. Des. 146 (2019) 1805–1809, https://doi.org/10.1016/j.fusengdes.2019.03.040.
[4] https://www.babcock.com.
[5] J.B. Kitto, S.C. Stultz, Steam, Its Generation and Use, 41st ed., The Babcock & Wilcox Company, 2005.
[6] US Nuclear Regulatory Commission, Pressurized water reactor B&W technology, crosstraining course manual, Chapter 2.4, once-through steam generator. Available online at: https://www.nrc.gov/docs/ML1122/ML11221A117.pdf.
[7] The Babcock & Wilcox Company, Thermal-Hydraulic Analysis of Once-Through Steam Generators, EPRI N P-1431 Project S131-1 Final Report, Alliance, Ohio, 1980. Available at: https://www.osti.gov/servlets/purl/5262028.
[8] A. Tincani, et al., Conceptual design of the steam generators for the EU DEMO WCLL Reactor, Energies 16 (6) (2023), 2601. 10.3390/en16062601.
[9] USNRC. RELAP5/MOD3 code manual volume I: code structure, system models, and solution methods, NUREG/CR-5535, Washington DC., 1998.
[10] C. Ciurluini, et al., Analysis of the thermal-hydraulic behavior of the EU-DEMO WCLL breeding blanket cooling systems during a loss of flow accident, Fusion Eng. Des. 164 (2021), 112206, https://doi.org/10.1016/j.fusengdes.2020.112206.
[11] C. Ciurluini, et al., Study of the EU-DEMO WCLL breeding blanket primary cooling circuits thermal-hydraulic performances during transients belonging to LOFA category, Energies 14 (6) (2021) 1541, https://doi.org/10.3390/en14061541.
[12] F. Galli, et al., Evaluation of the thermal-hydraulic performances of a once-through steam generator in nuclear fusion applications, J. Phys. Conf. Ser. 2177 (2022), 012017, https://doi.org/10.1088/1742-6596/2177/1/012017.
[13] F. Mascari, et al., Sensitivity analysis of the MASLWR helical coil steam generator using TRACE, Nucl. Eng. Des. 241 (4) (2011) 1137–1144, https://doi.org/10.1016/j.nucengdes.2010.05.002.
[14] A. Tarallo, et al., Preliminary mechanical design of the once-through steam generators for the EU DEMO WCLL breeding blanket concept, in: Proceedings of the 32nd Symposium on Fusion Technology (SOFT), Dubrovnik, Croatia, 2022, 18th –23rd September.
[15] I.E. Idelchik, Handbook of Hydraulic Resistance, 4th ed., Begell House, Inc., 2007. ISBN 978-1567002515.
[16] A.M. Spontarelli, CFD analysis of the aspirator region in a B&W enhanced once-through steam generator, Master degree Thesis, Blacksburg, Virginia, 2013, available online at: https://vtechworks.lib.vt.edu/handle/10919/23182.
[17] R.R. Clark Jr., Modeling two-phase flow in the downcomer of a once-through steam generator using RELAP5/MOD2, Master degree Thesis, Blacksburg, Virginia, 2011, available online at: https://vtechworks.lib.vt.edu/bitstream/handle/10919/76861/etd-01092012-145824_Clark_RR_T_2011.pdf?sequence=1.
[18] The US Nuclear Regulatory Commission (USNRC), RELAP5/MOD3.3 code manual volume 2, appendix A: input requirements, NUREG/CR-5535; USNRC: Washington, DC, USA, 1995.
[19] F.P. Incropera, et al., Fundamentals of Heat and Mass Transfer, 7th Ed, John Wiley & Sons Inc., Hoboken, New Jersey, USA, 2011.
[20] The American Society of Mechanical Engineers (ASME), Boiler and pressure vessel code, Section II, Part D, properties (metric), 2015 Edition, New York, New York, USA.
[21] ISOVER® Saint-Gobain Manufacturing Company, TECH Telisol 5.0 QN technical datasheet. ISOVER-TDS-Industry-INT-ENG-TECH Telisol 5.0 QN 2019-09. Available online at: https://www.isover-technical-insulation.com/products/tech-telisol-50-qn#children-attributes-table.
[22] A. Vannoni, et al., Development of a steam generator mock-up for EU DEMO fusion reactor: conceptual design and code assessment, in: Proceedings of the 32nd Symposium on Fusion Technology (SOFT), Dubrovnik, Croatia, 2022, 18th –23rd September.